



# Characterizing soil thermal conductivity in situ: development of a novel cone penetration test module

J. Bindner<sup>\*1</sup>, O. Siau-Hwa<sup>1</sup>, E. Cargill<sup>1</sup>, Y.N. Byrne<sup>2</sup>, R. Dolling<sup>1</sup>, K. Cabal<sup>1</sup>, J. Hobbs<sup>2</sup>  
*ConeTec Group<sup>1</sup>, Lankelma<sup>2</sup>*

<sup>\*</sup>Joseph.Bindner@conetec.com

**ABSTRACT:** Understanding soil thermal conductivity is essential for the design of buried energy transmission cables. The thermal conductivity of soils can be characterized ex situ using soil samples, which may result in sample disturbance and is time- and labor-intensive. For these reasons, in situ methods that characterize soil thermal conductivity are generally preferred, especially if they can be performed simultaneously with the commonly used cone penetration test (CPT). Recent advancements in CPT-compatible thermal characterization methods include the heat flow CPT and the thermal CPT, which both show promise for the characterization of soil thermal conductivity in situ. However, the characterization of thermal conductivity using CPT-compatible methods is still an emerging field with limited available options. As a result, exploring alternative methods serve to enhance scientific understanding and contribute new methodologies to this field of study. The objective of this study is to create an alternative method for the measurement of in situ soil thermal conductivity by developing a CPT module that measures soil thermal conductivity in a manner that is similar to the thermal needle probe. The patent pending thermal module includes a copper rod imbedded in the side of a CPT push rod to monitor heat dissipation in soils, similar to the thermal needle probe. The calibration method for the thermal module is outlined and in situ thermal module measurements at three sites (33 test depths) are compared against paired thermal needle probe measurements on undisturbed samples. Results indicate the thermal module captures the trend in thermal conductivity for a range of soil conditions and shows promise for the characterization of soil thermal conductivity with a mean bias error of 0.23 W/mK.

**Keywords:** Thermal Conductivity; Cone Penetration Test; Site Investigation

## 1 INTRODUCTION

The design of buried infrastructure that emits heat, such as current transmission cables, requires consideration of environmental factors to prevent overheating. Effective design of these systems hinges on understanding the rate at which soils dissipate heat, particularly in offshore environments where buried infrastructure is increasingly common. Soil thermal conductivity ( $\lambda$ ) is a geotechnical characteristic which describes a material's ability to transfer heat and is influenced by mineralogy, density, and moisture content (IEEE Standards Association, 2017).

Thermal conductivity is commonly measured on undisturbed samples using methods such as the thermal needle probe (ASTM International, 2022). However, undisturbed samples are generally only obtained for fine grained soils, obtaining high quality samples may not always be feasible, and sampling and testing is generally time and labor intensive.

In situ methods that measure thermal conductivity are generally more cost effective and include direct push applications of the thermal needle probe, among other methods (Vrielink et al., 2024). However, many in situ methods are not compatible with the commonly used cone penetration test (CPT). CPT-compatible

methods for the in situ measurement of thermal conductivity include the thermal cone penetration test (T-CPT) (a.k.a. thermal cone dissipation test) (Akrouh et al., 2016; Lines et al., 2017; Liu et al., 2021; Mo et al., 2021; Mo et al., 2022; Vardon et al., 2019; Vardon & Peuchen, 2021) and the Heat Flow Cone Penetration Test (HF-CPT) (Isaev et al., 2018; Vrielink et al., 2023). The T-CPT includes temperature sensors and, in some cases a heating element, to provide the capability to conduct the CPT and thermal testing at a single sounding location. Additionally, the HF-CPT includes a CPT module with heating elements and temperature sensors for the characterization of soil thermal conductivity. While these methods show promise, the use of CPT-compatible techniques to measure soil thermal conductivity remains an emerging practice. Research that introduces new tools is important for advancing our understanding of how different methods perform for the measurement of soil thermal conductivity in situ.

The objective of this study is to create a CPT module for the in situ measurement of soil thermal conductivity that resembles an embedded thermal needle probe. This paper presents the design, calibration, and field testing of a patent pending thermal module for the in situ characterization of soil

thermal conductivity. The presented thermal module is CPT-compatible and was deployed at three test sites. In situ measurements from the thermal module are compared against the commonly used thermal needle probe and results show promise for the characterization of soil thermal conductivity using the novel CPT module.

## 2 METHODS AND MATERIALS

### 2.1 Thermal Module Design

Figure 1a displays an image of the thermal module prototype, which is designed to be used in-line with standard CPT equipment. The diameter of the thermal module is compatible with the 15 cm<sup>2</sup> CPT. The key elements of the module include (1) a partially exposed copper rod (5 mm diameter by 160 mm length), (2) an internal heating element in contact with the copper rod, (3) a sensor to monitor the temperature of the copper rod, (4) low thermal conductivity plastic near the copper rod for thermal insulation, and (5) an outer metal housing that connects the thermal module to up-hole push rods and down-hole CPT equipment (41 cm in length). The thermal module measures soil thermal conductivity based on similar concepts to the needle probe method.

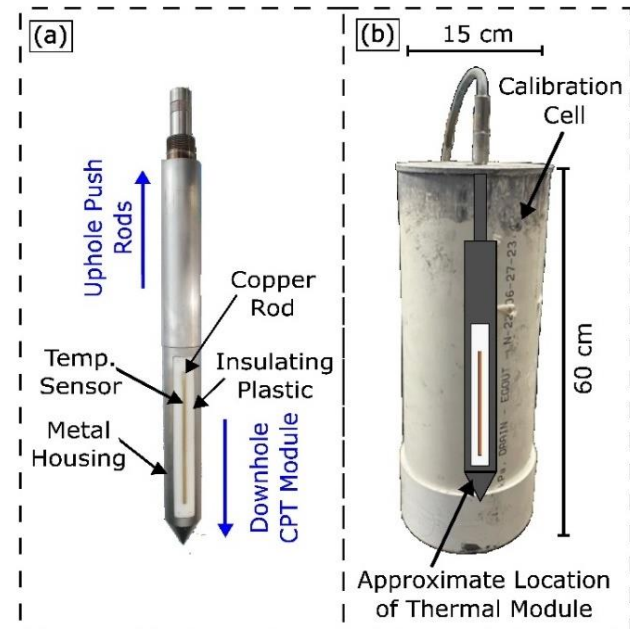


Figure 1. (a) Thermal CPT module with primary elements labelled including the copper rod, the insulating plastic substrate, the metal module housing, and the location of the temperature sensor. Push rods are located up-hole of the thermal module and the CPT unit is attached downhole of the thermal module. (b) Image of the calibration cell with the approximate location of the thermal module during testing displayed (profile view).

### 2.2 Thermal Module Calibration

Unlike the thermal needle probe, the thermal module calibration model cannot be expressed with a simple analytical equation. Therefore, calibration is required to correlate thermal dissipation data to thermal conductivities. Figure 1b displays the testing setup used for module calibration including the calibration cell and approximate location of thermal module (with dummy cone tip) during calibration. The dimensions of the calibration cell are shown in Figure 1b and were selected to ensure boundary effects were negligible. Thermal module calibration was performed using a synthetic paste-like material (calibration material). The thermal conductivity of the calibration material was measured using a Thermtest portable thermal conductivity needle probe (TLS-100 with 150 mm probe) which reports an accuracy of  $\pm 5\%$  and reproducibly of  $\pm 2\%$  for soils (Thermtest Portable, n.d.). The calibration material was placed in the calibration cell and the thermal module was inserted. After insertion, the module temperature was monitored until the instrument reached thermal equilibrium. The power supply to the heating element was then set to a constant power, turned on, and the change in temperature of the copper rod was recorded for 5 minutes.

Figure 2 displays the thermal dissipation curve for the thermal module in a calibration material with a  $\lambda = 0.92 \text{ W/mK}$ . The rate of temperature change in Phase 1 corresponds to the initial heating of the copper rod (Figure 2). The quasi-steady state temperature change in Phase 2 is dominated by the thermal properties of the calibration material (Figure 2) (ASTM International, 2022). The power to the thermal module was selected to reduce the signal to noise ratio while adequately developing the quasi-steady state condition and limiting the effect of moisture migration.

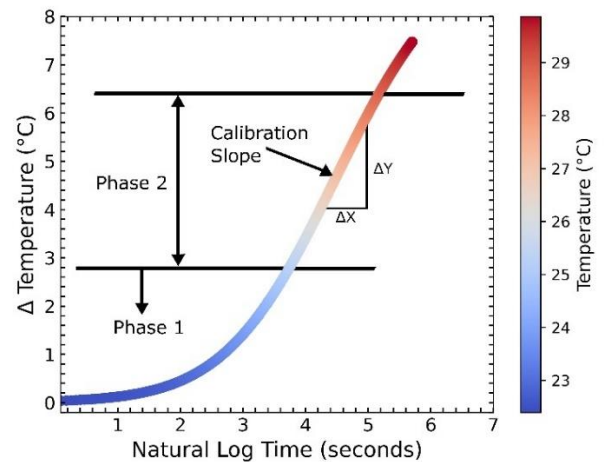


Figure 2 – Thermal module temperature change over time during module heating. The thermal dissipation data was collected during module calibration in a material with a thermal conductivity of  $0.92 \text{ W/mK}$ .

Figure 3 displays 11 calibration test dissipation slopes plotted against the TLS-100 measured thermal conductivity of each calibration material. An exponential function was used to represent the calibration model. The calibration model does not account for variations in soil volumetric heat capacity ( $C_v$ ) compared to the calibration material's  $C_v$ , which introduces uncertainty to the calibration. Finite element analyses were completed to assess the impact of volumetric heat capacity variation on calibration model performance and was found to introduce up to 3% error in reported  $\lambda$ . Details on finite element analysis are not included in the scope of this paper.

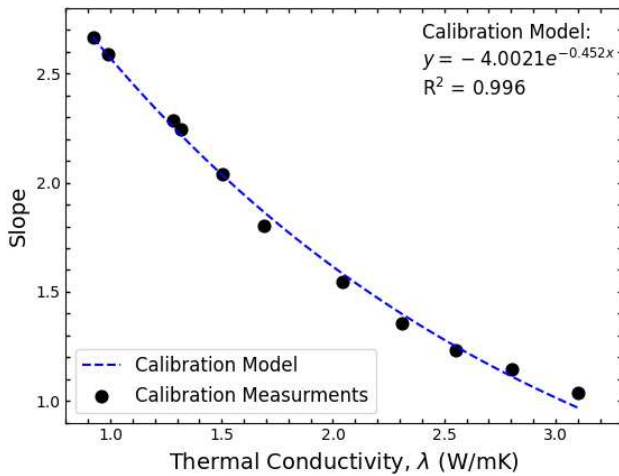


Figure 3 – Results from thermal module calibration testing including the calibration slopes plotted against the thermal conductivity of the calibration material. The calibration model is described by an exponential function.

### 2.3 In Situ Geotechnical Validation

The thermal module underwent a series of field tests to assess the in situ performance of the instrument compared to thermal needle probe measurements on undisturbed samples. Figure 4 displays three test sites, located in the continental United States, that were selected based on the range of soil conditions present at these sites, based on normalized soil behavior type (SBTn) (Robertson, 2009) (Figure 5). At each test site, the SBTn was first characterized using the CPT at two locations approximately 5-10 meters apart. Results from the CPT soundings were used to identify testing depths with diverse SBTn that were located below the water table. A total of 33 testing depths were selected between the three sites. **Erreur ! Source du renvoi introuvable.** displays the SBTn of soils at the selected testing depths. Testing in Seattle, Washington, was conducted to a depth of approximately 12 m below ground surface (BGS) and soils at test depths predominantly classified as sensitive fine-grained soils, silt mixtures, and sand mixtures, with one depth

classifying as sand (Figure 5). Tests in Salt Lake City were performed to a depth of approximately 20 m BGS and were dominated by silt mixtures and sand mixtures (Figure 5). Thermal module testing near San Francisco was performed to a depth of approximately 22 m BGS in soils that predominantly behaved as clays and silt mixtures (Figure 5).



Figure 4 – Map displaying the three test sites located in the continental United States including locations near Seattle, WA, San Francisco, CA, and Salt Lake City, UT.

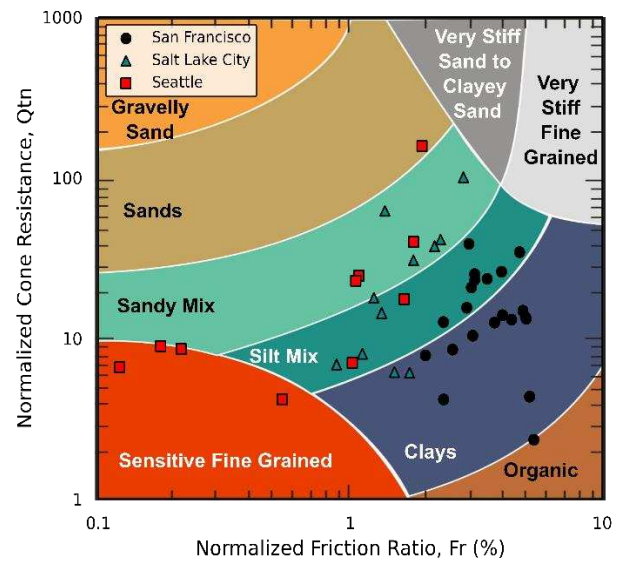


Figure 5 – Normalized soil behaviour type (SBTn) for the soils at each thermal module test depth.

At each test location, the thermal module with a dummy tip was advanced to the desired testing depth and the thermal testing procedure used for instrument calibration was repeated, including thermal equilibration and a 5-minute testing period. Recorded data were used to determine the Phase 2 slope of the thermal dissipation plot. The calibration model was then used to determine  $\lambda$ .

To assess the performance of thermal module  $\lambda$  measurements, the TLS-100 was used to measure the thermal conductivity of undisturbed samples collected



at each thermal module testing depth and within 5 meters, horizontally. Undisturbed samples were collected using 7.6 cm (3 inch) diameter thin-walled samplers (Shelby tubes). Drilling methods for undisturbed sampling included hollow stem auger and mud rotary drilling. Measurements collected using the TLS-100 were taken in general accordance with ASTM D5334-22 (ASTM International, 2022).

### 3 RESULTS

Figure 6 displays a representative thermal dissipation plot for data collected in the field. The general shape of the field temperature dissipation curve is similar to those from thermal module calibration. The quasi-steady state slope of field temperature dissipation plots was used to calculate  $\lambda$ , using the calibration model, and yielded thermal conductivity values within the expected range for clayey saturated soil (1 to 2 W/mK) (Bai and Bai, 2012).

Figure 7 displays the cone resistance, sleeve friction, water table, and soil behaviour type from CPT testing plotted next to thermal conductivity results from the thermal module and the TLS-100 for one of the testing locations in San Francisco. Results illustrate lower thermal conductivity for clays, moderate thermal conductivity for silt mixtures, and higher thermal conductivity for sand mixtures, respectively.

Figure 8 displays the reference  $\lambda$  measurements using the TLS-100 plotted against  $\lambda$  measurements using the thermal module. Points plotted in the dark gray shaded region have precision within 15% of the overall trend and points within the light gray area have precision within 30%. The majority of tests have precisions within 15% of the trend line. Results from all sites yield a root mean squared error (RMSE) of 0.28 W/mK. Thermal module measurements are generally greater than TLS-100 measures, with a mean bias error (MBE) of 0.23 W/mK. The variability of  $\lambda$  is generally captured by thermal module measurements, as illustrated by the trendline in Figure 8. Most measurements collected using the thermal module were within 0.5 W/mK of the TLS-100 measurements.

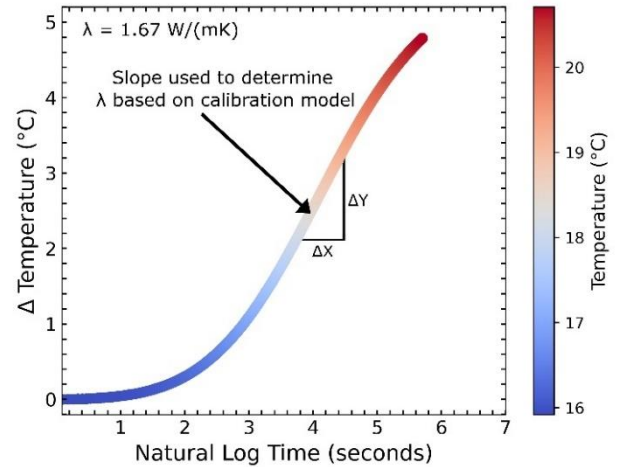


Figure 6 – Example results from thermal module testing in saturated clayey soils at a depth of 8.4 m below ground surface. The slope of the linear portion of data was converted to thermal conductivity using the calibration model.

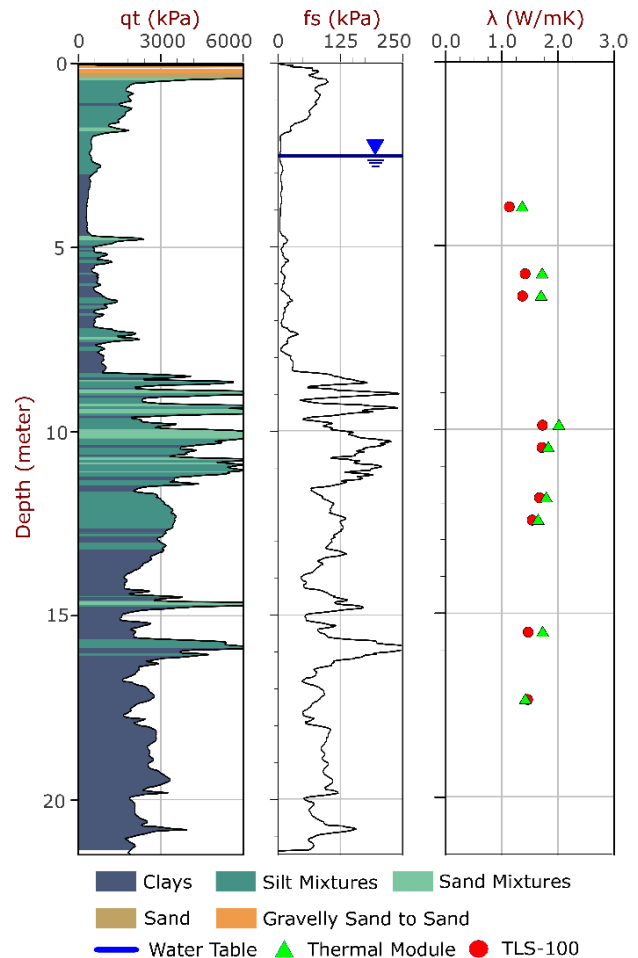


Figure 7 – CPT plot for testing near San Francisco, CA. Results include the CPT cone resistance ( $qt$ ) and soil behaviour type from Robertson (2009 & 2010), sleeve friction ( $fs$ ), dynamic pore water pressure ( $u$ ), and thermal conductivity from the thermal module and TLS-100.

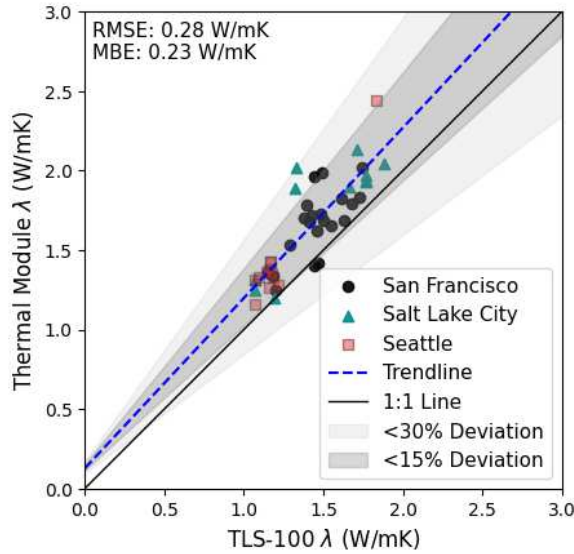


Figure 8 – Results of field testing at the three test sites including the root mean squared error and mean bias error. Shaded gray regions display the regions where data deviation from the overall trendline is within  $\pm 15\%$  and  $\pm 30\%$  of the trendline.

#### 4 DISCUSSION

Observations from the thermal module field results suggest thermal conductivity variability by soil type is captured, with fine-grained soils having lower thermal conductivity than sandy soils. The positive MBE of thermal module measurements is hypothesized to be associated with improved soil contact with the thermal module in situ compared to TLS-100 measurements on undisturbed samples and the potential for reduced moisture conditions of undisturbed samples, resulting in higher measures of thermal conductivity in situ. However, future research is needed to better understand why the thermal module results in greater measures of thermal conductivity compared to the thermal needle probe.

Results also illustrate that most measurements of thermal conductivity using the thermal module are within  $\pm 15\%$  deviation from the trendline, which is similar to measurements using the thermal needle probe. (Hust & Smith, 1989) compared the interlaboratory measurements of thermal conductivity, using the thermal needle probe, and reported a precision of  $\pm 10\%$  to  $\pm 15\%$  for Ottawa silica sand and paraffin wax, which have thermal conductivities similar to the soils in this study.

While results indicate the thermal module shows promise for the characterization of soil thermal conductivity, the authors acknowledge limitations of this study. Although this study is applicable to onshore soils below the water table, the depositional environment, soil mineralogy, and effective stress

conditions in marine environments may vary. Future work is needed to understand how the thermal module prototype performs in marine environments. Additionally, the calibration model used in this study was selected for simplicity and reasonable fit for the range of calibration data. However, future work should consider moving to a calibration model that more closely represents a physics informed heat transfer model and includes more calibration points. Also, the thermal needle probe was used to measure the thermal conductivity of the calibration material, and the TLS-100 has some level of uncertainty in measurements. Variability in the thermal module measurements may be related to variability in thermal needle probe via calibration. Additionally, future studies should explore the harshness of conditions this tool can be exposed to without compromising the quality of measurements.

#### 5 CONCLUSIONS

The objective of this study was to create a novel instrument for the measurement of soil thermal conductivity that is compatible with CPT equipment. A CPT-compatible thermal module was created and the instrument was calibrated for a range of thermal conductivities. Three testing locations in the continental United States were selected to assess the performance of the thermal module in a range of soil conditions. Thirty-three testing depths were selected across the test sites for comparison to reference measurements using the thermal needle probe.

Measurements of thermal conductivity using the thermal module resulted in an RMSE of  $0.28 \text{ W/mK}$  and an MBE of  $0.23 \text{ W/mK}$ . When comparing the thermal conductivity measurements from the thermal needle probe method and the thermal module, results are typically within  $15\%$  of the trendline presented in Figure 8.

Results from this study suggest that the thermal module prototype shows promise for the in situ characterization of soil thermal conductivity. The instrument is compatible with CPT equipment making the cost-effective capture of soil thermal conductivity and soil behaviour in a single sounding possible.

The initial geotechnical validation of this instrument requires further testing to understand how this tool performs in offshore soil conditions. Future studies should consider alternative calibration models, assess how the instrument performs in a broader range of soil conditions including unsaturated soils, and assess how reference measurement accuracy impacts the reported instrument performance.

## AUTHOR CONTRIBUTION STATEMENT

**J. Bindner:** Data curation, Formal analysis, Methodology, Visualization, Writing – original draft; **O. Siau-Hwa:** Conceptualization, Data curation, Formal analysis, Investigation, Methodology, Software, Writing – original draft; **E. Cargill:** Conceptualization, Project administration, Resources, Supervision, Writing – review & editing; **Y. Byrne:** Data curation, Formal analysis, Conceptualization, Writing – original draft; **R. Dolling:** Conceptualization, Project administration, Resources, Supervision, Writing – review & editing; **K. Cabal:** Validation, Writing – review & editing; **J. Hobbs:** Validation, Writing – review & editing.

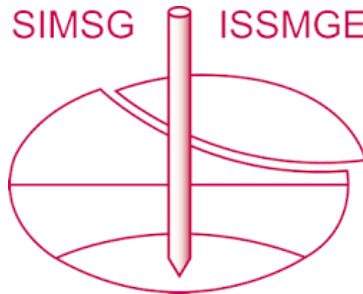
## ACKNOWLEDGEMENTS

The authors gratefully acknowledge: Thanh Nguyen for her contributions to calibration of the instrument; Randy Hu for support of the module mechanical design; Peter Bowen for his contributions to field work; Iman Entezari and Dallas McGowan for their technical guidance.

## 6 REFERENCES

- Akrouh, G. A., Briaud, J.-L., Sanchez, M., & Yilmaz, R. (2016). Thermal Cone Test to Determine Soil Thermal Properties. *Journal of Geotechnical and Geoenvironmental Engineering*, 142(3), 04015085. [https://doi.org/10.1061/\(ASCE\)GT.1943-5606.0001353](https://doi.org/10.1061/(ASCE)GT.1943-5606.0001353)
- ASTM International. (2022). *Standard Test Method for Determination of Thermal Conductivity of Soil and Rock by Thermal Needle Probe Procedure*. ASTM International. <http://www.astm.org/>
- Hust, J. G., & Smith, D. R. (1989). *Interlaboratory comparison of two types of line-source thermal-conductivity apparatus measuring five insulating materials* (NIST IR 89-3908; 0 ed., p. NIST IR 89-3908). National Institute of Standards and Technology. <https://doi.org/10.6028/NIST.IR.89-3908>
- IEEE Standards Association. (2017). *IEEE Guide for Thermal Resistivity Measurements of Soils and Backfill Materials*. IEEE. <https://doi.org/10.1109/IEEESTD.2018.8353815>
- Isaev, O. N., Sharafutdinov, R. F., & Zakatov, D. S. (2018). Thermophysical finite element analysis of thawing of frozen soil by means of HT-CPT cone penetrometer. *Cone Penetration Testing 2018 - Hicks, Pisanò & Peuchen* (Eds), 365–370.
- ISO. (2015). ISO 17628:2015: Geotechnical investigation and testing - Geothermal testing - Determination of thermal conductivity of soil and rock using a borehole heat exchanger.
- Lines, S., Williams, D. J., & Galindo-Torres, S. A. (2017). Determination of Thermal Conductivity of Soil Using Standard Cone Penetration Test. *Energy Procedia*, 118, 172–178. <https://doi.org/10.1016/j.egypro.2017.07.036>
- Liu, X., Surya Sarat Chandra Congress, Guojun Cai, Lulu Liu, Songyu Liu, Anand J. Puppala, & Wenwei Zhang. (2021). Development and validation of a method to predict the soil thermal conductivity using thermal piezocone penetration testing (T-CPTU). *Canadian Geotechnical Journal*, 59(4). <https://doi.org/10.1139/cgj-2021-0034>
- Mo, P. Q., Gao, L., Yu, H. S., Tao, X. L., & Ma, Q. Z. (2022). Physical and numerical modelling of T-CPT for mechanisms of penetration and heat transfer. In L. Tonni & G. Gottardi, *Cone Penetration Testing 2022* (1st ed., pp. 577–583). CRC Press. <https://doi.org/10.1201/9781003308829-83>
- Robertson, P. K. (2009). Interpretation of cone penetration tests—A unified approach. *Canadian Geotechnical Journal*, 46(11), 1337–1355. <https://doi.org/10.1139/T09-065>
- Robertson, P. K. (2010). *Soil behaviour type from the CPT: an update*.
- Thermtest Portable. (n.d.). *TLS-100 Portable Meter-User Manual*. Thermtest Portable.
- Vardon, P. J., Baltoukas, D., & Peuchen, J. (2019). Interpreting and validating the thermal cone penetration test (T-CPT). *Géotechnique*, 69(7), 580–592. <https://doi.org/10.1680/jgeot.17.P.214>
- Vardon, P. J., & Peuchen, J. (2021). CPT correlations for thermal properties of soils. *Acta Geotechnica*, 16(2), 635–646. <https://doi.org/10.1007/s11440-020-01027-2>
- Vrielink, L., Parasie, N., Peuchen, J., Daniilidis, A., & Vardon, P. J. (2023). Development of the heat flow cone penetration test (HF-CPT). *Symposium on Energy Geotechnics 2023*, 1–2. <https://doi.org/10.59490/seg.2023.606>
- Vrielink, L., Peuchen, J., & Parasie, N. (2024). In Situ Test Methods for Thermal Site Characterisation – A Comparison. *7th International Conference on Geotechnical and Geophysical Site Characterization*. 7th International Conference on Geotechnical and Geophysical Site Characterization. <https://doi.org/10.23967/isc.2024.013>

# INTERNATIONAL SOCIETY FOR SOIL MECHANICS AND GEOTECHNICAL ENGINEERING



*This paper was downloaded from the Online Library of the International Society for Soil Mechanics and Geotechnical Engineering (ISSMGE). The library is available here:*

<https://www.issmge.org/publications/online-library>

*This is an open-access database that archives thousands of papers published under the Auspices of the ISSMGE and maintained by the Innovation and Development Committee of ISSMGE.*

*The paper was published in the proceedings of the 5th International Symposium on Frontiers in Offshore Geotechnics (ISFOG2025) and was edited by Christelle Abadie, Zheng Li, Matthieu Blanc and Luc Thorel. The conference was held from June 9<sup>th</sup> to June 13<sup>th</sup> 2025 in Nantes, France.*